THE JOURNAL OF PHYSICAL CHEMISTRY Letters

Letter

pubs.acs.org/JPCL

Controlling Catalytic Selectivities during CO_2 Electroreduction on Thin Cu Metal Overlayers

Rulle Reske,[†] Matteo Duca,[‡,⊥] Mehtap Oezaslan,[†,§] Klaas Jan P. Schouten,[⊥] Marc T. M. Koper,[⊥] and Peter Strasser*[,†]

[†]Department of Chemistry, Chemical Engineering Division, Technical University Berlin, 10623 Berlin, Germany

[‡]Laboratoire d'Electrochimie Moléculaire, Unité Mixte de Recherche Université−CNRS no. 7591, Université Paris Diderot, Sorbonne Paris Cité, Bâtiment Lavoisier, 15 Rue Jean de Baïf, 75205 Paris Cedex 13, France

[§]The Electrochemistry Group, Paul Scherrer Institut, 5232 Villigen, PSI, Switzerland

[⊥]Leiden Institute of Chemistry, Leiden University, Einsteinweg 55, P.O. Box 9502, 2300 RA Leiden, The Netherlands

Supporting Information

ABSTRACT: The catalytic activity and selectivity of the electrochemical CO_2 reduction on Cu overlayers with varying atomic-scale thickness on Pt was investigated. Hydrogen, methane, and ethylene were the main products. Beyond an activity improvement with increasing copper layer thickness, we observed that the thickest 15 nm Cu layer behaved bulk-like and resulted in high relative faradaic selectivities for hydrocarbons. With decreasing Cu layer thickness, the formation of methane decreased much faster than that of ethylene. As a result, the relative faradaic selectivity of the technologically useful product ethylene increased sharply. The selectivity ratios between methane and ethylene were independent of electrode potential on a Cu monolayer. A combination of geometric tensile strain effects and electronic effects is believed to control the surface reactivity and product distribution on the copper surfaces. This study highlights the general strategy to tune product distributions on thin metal overlayers.

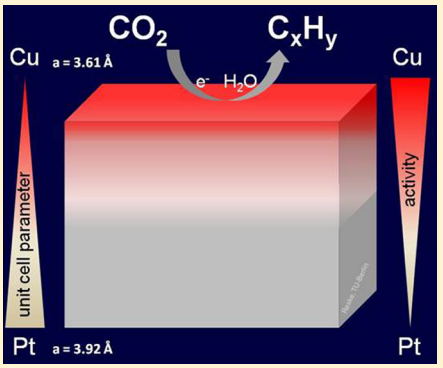

SECTION: Energy Conversion and Storage; Energy and Charge Transport

The efficient large-scale conversion of excess renewable electricity into useful chemicals or fuels via low-energy molecules has attracted great attention in academia and the chemical industry. A prominent example of low-energy waste molecules is carbon dioxide, CO_2, which is produced in large amounts in exhaust gas of concrete production plants or power plants. Improvements in activity, selectivity, and durability for (electro)catalysts are of general interest to enhance the economic competitiveness of catalytically industrial processes.

The electrochemical conversion of CO_2 on different extended monometallic surfaces has been frequently investigated.[1−3] However, the mechanism is poorly understood to date due to the multiple highly complex proton- and electron-transfer steps. It is widely accepted in the literature that carbon monoxide is the adsorbed intermediate species on the copper surface during the CO_2 electroreduction to generate hydrocarbon products such as methane and ethylene.[4−8] Compared to other metals, the high activity on Cu is attributed to the intermediate heat energy of adsorption of CO species (H_{ad} = 71 kJ mol^{-1}).[1,9−11] Although copper shows reactivity for the electroreduction of CO_2, strategies to tune product selectivity are missing. In general, the surface reactivity and selectivity can be easily changed by short-range electronic and geometric effects.[12−15] Due to the lattice mismatch between the metal overlayer and substrate, the strain effects have been used to alter the adsorption energy of the reactive surface intermediate.[16−18] In this work, we show that Cu overlayers of varying thickness supported on Pt can be used to control the product selectivity of the CO_2 reduction reaction. We prepared nanometer-scale thin Cu layers deposited on platinum and monitored their resulting catalytic CO_2 reduction reactivity and selectivity as a function of the electrode potential. The altered surface reactivity and product distribution are believed to be induced by strain and electronic effects.

Figure 1a shows baseline-corrected normalized mass spectrometric ion current signals of H_2 (m/z = 2), CH_4 (m/z = 15), and C_2H_4 (m/z = 26) produced by CO_2 electroreduction on Pt (polycrystalline (pc)), the Cu monolayer (Cu_{ML}/Pt), the 5 nm (Cu_{5nm}/Pt), and the 15 nm (Cu_{15nm}/Pt) Cu layer as a function of the applied potential. Figure 1d shows the corresponding cathodic current−potential scans for all overlayer catalysts as well as a standard bulk polycrystalline copper electrode at a scan rate of 1 mV/s. It is evident from Figure 1a that pure platinum shows highly exclusive activity for the hydrogen evolution but no activity for the CO_2 reduction (see Figure S7, Supporting Information). Hydrogen formation

Received: May 27, 2013
Accepted: July 9, 2013
Published: July 9, 2013

   dx.doi.org/10.1021/jz401087q | J. Phys. Chem. Lett. 2013, 4, 2410−2413

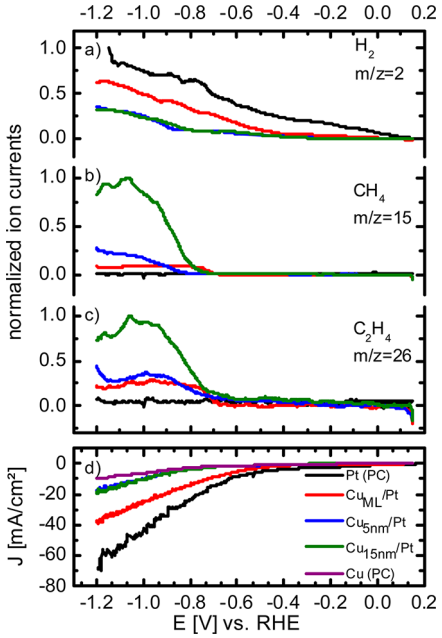

Figure 1. (a–c) The normalized ion currents for hydrogen, methane, and ethylene probed by in situ OLEMS (online electrochemical mass spectrometry) in dependence of the applied cathodic potential and (d) polarization curves for CO_2 electroreduction on different nanometer-scaled layer thicknesses of Cu supported on pure Pt in 0.1 M $KHCO_3$ at room temperature.

decreases while hydrocarbon formation increases with increasing thickness of the Cu deposit. Beyond the Cu layer thickness of 5 nm, hydrogen evolution approaches Cu-like I–E values.

Moreover, the onset potential of the hydrogen evolution reaction (HER) clearly shifted to more cathodic potentials compared to pure bulk platinum. The following onset potentials were detected E = 0.06 V, −0.43 V, and −0.47 V for pure platinum, 1 ML of Cu, and 5 nm or 15 nm bulk copper layers, respectively. It is noted that with one copper monolayer, the onset potential for HER was shifted by 490 mV compared to that of pure Pt. This observation supports the presence of a closed Cu (1 × 1) layer on top of the Pt substrate and evidences the drastic effect of a single atomic overlayer of Cu on the hydrogen adsorption and evolution reaction. The formation of methane and ethylene in dependence of the electrode potential are plotted in Figure 1b and c. The mass spectrometric data reveal that with increasing Cu thickness, the formation of methane and ethylene increases. The Pt substrate appears to exert a detrimental influence on surface adsorption and reaction characteristics of thin Cu overlayers. The onset potential of methane formation is also affected by the thickness of the copper layer. While the onset potentials were similar for Cu_{5nm}/Pt and Cu_{15nm}/Pt, the Cu_{ML}/Pt shows a shift of around 100 mV to more positive potentials (see Table 1). The low hydrocarbon formation activity of the Cu monolayer indicates a strong electronic and geometric effect of the Pt substrate on the resulting adsorption and reactivity of CO_2 and its intermediates. In contrast, the onset potentials for ethylene varied merely in the range of 30 mV between the monolayer and the thicker layers. The production of ethylene on Cu_{5nm}/Pt was only slightly higher than that on Cu_{ML}/Pt. The decreasing intensities for methane and ethylene on the $Cu_{15\ nm}$/Pt at E = −1.06 V are likely caused by deactivation of the copper surface by impurities, as found earlier.[6,19]

Table 1. Onset Potentials for Hydrogen, Methane, and Ethylene on Various Nanometer-Scaled Layer Thicknesses of Copper Deposited on Polycrystalline Platinum

	Pt	Cu_{ML}	Cu_{5nm}	Cu_{15nm}
$E_{onset}(H_2)$ [V] vs RHE	0.06	−0.43	−0.47	−0.47
$E_{onset}(CH_4)$ [V] vs RHE		−0.71	−0.82	−0.79
$E_{onset}(C_2H_4)$ [V] vs RHE		−0.69	−0.72	−0.72

The nature and selectivities of the reaction products of the electrocatalytic CO_2 reduction depend sensitively on the nature and geometry of the catalytic metal surface.[20−23] On Cu and Pt, major chemical products are hydrogen, methane, and ethylene. Minor products are CO and formic acid.[1−3] We converted the OLEMS ion currents into relative faradaic selectivities (RFSs) of methane, ethylene, and hydrogen according to eq S8 (Supporting Information) assuming a linear relationship between the ion current and the molar formation rate in the product gas. RFSs of methane and ethylene are shown for the three Cu/Pt catalysts between E = −0.8 V and −1.1 V in Figure 2. The hydrocarbon RFS values decreased sharply in the order

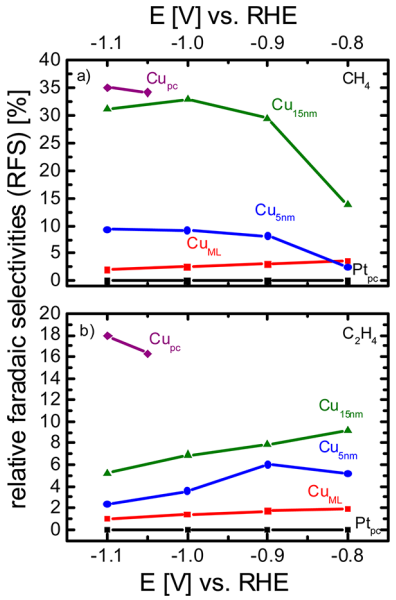

Figure 2. Relative Faradaic Selectivities (RFS) for (a) CH_4 and (b) C_2H_4 on different layer thicknesses of Cu deposited on Pt polycrystalline during the CO_2 electroreduction in 0.1 M $KHCO_3$ at room temperature. Polycrystalline copper is added as a reference.

Cu_{15nm}/Pt > Cu_{5nm}/Pt > Cu_{ML}/Pt. The highest RFS values were reached on polycrystalline copper in accordance with the Cu_{15nm}/Pt overlayer catalyst. Sweeping to more negative electrode potentials, the methane RFS increased on Cu_{5nm}/Pt and Cu_{15nm}/Pt by a similar factor, keeping their ratio essentially constant; see Figure 2a. Comparison with Figure 1d shows that this increase is in line with the higher overall faradaic current. The Cu_{ML}/Pt surface shows a different behavior. Here, the methane RFS values remained essentially constant over the considered potential range. In contrast, RFS values of ethylene decreased with a more negative electrode potential for all three Cu layer thicknesses (Figure 2b), again by a similar factor. The ethylene formation rate increases in the order of Cu_{ML}/Pt < Cu_{5nm}/Pt < Cu_{15nm}/Pt at any given potential. RFS values of ethylene on polycrystalline copper are 3 times higher than

dx.doi.org/10.1021/jz401087q | J. Phys. Chem. Lett. 2013, 4, 2410−2413

those on Cu_{15nm}/Pt. The observed potential dependence of the OLEMS currents and derived RFSs of ethylene and methane can be understood based on recent mechanistic studies of the CO_2 reduction reaction by DFT calculation. Peterson et al. predicted the protonation of CO to be the potential-limiting step in the methane formation.[5] At an electrode potential of $E = -0.74$ V, a computational prediction that is in reasonable agreement with our present experimental observations is that the CH_4 free-energy pathway becomes thermodynamically downhill. Methane formation increases steeply, as displayed in Figure 1b. Ethylene formation has been suggested to occur through a non-electrochemical C−C bond formation[5,24] or through an electron-mediated CO dimerization step, especially on Cu(100).[8] It is evident that the hydrocarbon selectivity decreases with decreasing copper layer thickness. This is consistent with the notion that ever thinner Cu layers lose their Cu identity and approach that of Pt, which is an ineffective hydrocarbon-producing catalyst.

We also analyzed product selectivity in terms of changes in the ratio of two selectivities. The selectivity ratios of methane and ethylene between −0.8 V and −1.1 V versus RHE are presented in Figure 3. The ratio of the RFS of methane

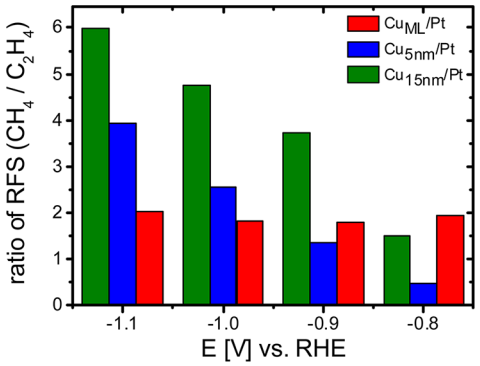

Figure 3. Ratios of RFSs for CH_4/C_2H_4 on different thicknesses of the Cu layer deposited on a pure Pt substrate obtained from the CO_2 reduction experiments in 0.1 M $KHCO_3$.

increases with a more negative potential for the Cu_{5nm}/Pt and Cu_{15nm}/Pt catalysts. On the Cu_{ML}/Pt, the selectivity of methane to ethylene is almost independent of the applied electrode potential. While the absolute ethylene formation rate drops from Cu_{15nm}/Pt to Cu_{ML}/Pt (see Figure 1c), its RFS is maximized for a single Cu overlayer, Figure 3. These trends in reactivity and selectivity of the CO_2 electroreduction on Cu overlayers are manifestations of more fundamental trends in electronic and geometric surface properties of the three catalysts. It is reasonable to assume that the surface adsorption energies of key reaction intermediates on the Cu_{ML}/Pt catalyst vary in such a way as to slow down the CO protonation of the methane pathway while favoring C−C bond formation and C_2H_4 production. With increasing thickness of the copper layer, the unit cell parameter decreases in the range from $a = 3.92$ Å to 3.61 Å for pure Pt and for pure Cu, respectively. The lattice mismatch between Cu and Pt atoms raises the interatomic distance of the copper atoms relative to that of pure bulk Cu and gives rise to tensile surface lattice strain effects that alter the adsorption energy of reactive intermediates. Furthermore, direct electronic interaction of Cu and Pt atoms in the monolayer catalyst affect adsorption of reaction intermediates as well. While the electronic effect decreases with increasing atomic distance and vanishes above a certain overlayer thickness, the tensile strain effect can remain effective over larger distances.[25] Thus, tensile strain may play a role for multiple Cu overlayers.

In conclusion, we have investigated the thickness effects of Pt-supported Cu overlayers on the catalytic activity and selectivity of CO_2 electroreduction. Clear correlations between thicknesses, activities and selectivities could be established for methane and ethylene as the most valuable products. The onset potential for methane on a single Cu monolayer shifts around 100 mV in comparison to that of more bulk-like Cu layers; however, the onset potential for ethylene remains nearly constant regardless of Cu thickness. The ratio of the RFSs for methane to ethylene can be controlled with the reduction potential and the copper layer thickness. The RFS of methane increases by increasing the Cu layer thickness as approaching a Cu bulk surface. It highlights that 1 ML of copper shows an almost constant ratio of the RFS for CH_4 to C_2H_4 over the potential range from −0.8 V to −1.1 V, with a better RFS for ethylene than that on the thicker Cu_{5nm}/Pt and Cu_{15nm}/Pt copper overlayers. The observed trends in reactivity and selectivity can be differences in surface strain, in particular, at multiple overlayers; strain alters chemisorption energies of reactive intermediates and can so later alter the preferred reaction pathways.

EXPERIMENTAL SECTION

A polycrystalline hemispherical platinum drop electrode with an electrochemically active surface area of 0.045 cm^2 (see Figure S1, Supporting Information) was used to deposit three Cu overlayers of different thicknesses by using under potential deposition (upd) and bulk copper deposition methods (see the Supporting Information for more details). Cu overlayer thicknesses studied are 1 ML and 5 and 15 nm. For the controlled deposition of a single Cu monolayer, the Cu deposition isotherm on polycrystalline Pt was established (see Figures S2 and S3, Supporting Information).[26,27] The deposition of one Cu monolayer was performed at a potential of 0.36 V for $t = 30$ s. For the bulk copper deposition, potentials of $E = 0.01$ V and 0.015 V versus RHE were applied for $t = 2$ s and 3 s, respectively, yielding Pt surfaces covered with 5 nm and 15 nm thick layers of Cu (see Figure S4, Supporting Information). Table S1 (Supporting Information) summarizes the calculated charges Q and the corresponding mean Cu layer thickness d (see eq S2, Supporting Information). Growth and structure of Cu overlayers on Pt have been reported frequently.[28−31] Cu forms epitaxial (1 × 1) monolayers on all three low-index facets.[29,30] Multilayers of Cu grow layer by layer in a (1 × 1) structure followed by three-dimensional cluster growth. While the lattice parameter of deposited copper on Pt(111) relaxes after the second layer to their bulk values, on Pt(100) and (110), the bulk lattice parameter is reached at 5−10 layers.[32−35] The structural, compositional, and morphological characterization of a 15 nm copper layer deposited on polycrystalline platinum is shown in Figures S5 and S6 (Supporting Information). The electrochemical CO_2 reduction experiments were performed in 0.1 M $KHCO_3$ electrolyte solution that had previously been saturated with argon and subsequently with CO_2 at room temperature (see the Supporting Information). The gaseous products hydrogen (H_2), methane (CH_4), and ethylene (C_2H_4) were analyzed in situ with an online electrochemical mass spectrometer

dx.doi.org/10.1021/jz401087q | J. Phys. Chem. Lett. 2013, 4, 2410−2413

(OLEMS) equipped with a tip that was positioned close to the working electrode (~10 μm).[36]

■ ASSOCIATED CONTENT

Supporting Information

Preparation of one copper monolayer, preparation of Cu bulk layer, experimental setup for CO_2 reduction, and calculation of relative faradaic selectivities. This material is available free of charge via the Internet at http://pubs.acs.org.

■ AUTHOR INFORMATION

Corresponding Author

*E-mail: pstrasser@tu-berlin.de.

Notes

The authors declare no competing financial interest.

E-mail: rulle.reske@tu-berlin.de (R.R.); matteo.duca@paris7.jussieu.fr (M.D.); mehtap.oezaslan@psi.ch (M.O.); kjp.schouten@chem.leidenuniv.nl (K.J.P.S.); m.koper@chem.leidenuniv.nl (M.T.M.K.).

■ REFERENCES

(1) Azuma, M.; Hashimoto, K.; Hiramoto, M.; Watanabe, M.; Sakata, T. *J. Electrochem. Soc.* **1990**, *137*, 1772.
(2) Hori, Y.; Takahashi, R.; Yoshinami, Y.; Murata, A. *J. Phys. Chem. B* **1997**, *101*, 7075.
(3) Gattrell, M.; Gupta, N.; Co, A. *J. Electroanal. Chem.* **2006**, *594*, 1.
(4) Hori, Y.; Murata, A.; Yoshinami, Y. *J. Chem. Soc., Faraday Trans.* **1991**, *87*, 125.
(5) Peterson, A. A.; Abild-Pedersen, F.; Studt, F.; Rossmeisl, J.; Norskov, J. K. *Energy Environ. Sci.* **2010**, *3*, 1311.
(6) Schouten, K. J. P.; Kwon, Y.; van der Ham, C. J. M.; Qin, Z.; Koper, M. T. M. *Chem. Sci.* **2011**, *2*, 1902.
(7) Kuhl, K. P.; Cave, E. R.; Abram, D. N.; Jaramillo, T. F. *Energy Environ. Sci.* **2012**, *5*, 7050.
(8) Schouten, K. J. P.; Qin, Z.; Gallent, E. P.; Koper, M. T. M. *J. Am. Chem. Soc.* **2012**, *134*, 9864.
(9) Somorjai, G. A. *Catal. Rev.: Sci. Eng.* **1978**, *18*, 173.
(10) Toyoshima, I. *Catal. Rev.: Sci. Eng.* **1979**, *19*, 105.
(11) Peterson, A. A.; Norskov, J. K. *J. Phys. Chem. Lett.* **2012**, *3*, 251.
(12) Mavrikakis, M.; Hammer, B.; Norskov, J. K. *Phys. Rev. Lett.* **1998**, *81*, 2819.
(13) Molodkina, E. B.; Ehrenburg, M. R.; Polukarov, Y. M.; Danilov, A. I.; Souza-Garcia, J.; Feliu, J. M. *Electrochim. Acta* **2010**, *56*, 154.
(14) Oezaslan, M.; Heggen, M.; Strasser, P. *J. Am. Chem. Soc.* **2012**, *134*, 514.
(15) Oezaslan, M.; Hasché, F.; Strasser, P. *Chem. Mater.* **2011**, *23*, 2159.
(16) Nilsson, A.; Pettersson, L. G. M.; Hammer, B.; Bligaard, T.; Christensen, C. H.; Norskov, J. K. *Catal. Lett.* **2005**, *100*, 111.
(17) Kitchin, J. R.; Norskov, J. K.; Barteau, M. A.; Chen, J. G. *J. Chem. Phys.* **2004**, *120*, 10240.
(18) Oezaslan, M.; Hasche, F.; Strasser, P. *J. Electrochem. Soc.* **2012**, *159*, B444.
(19) Hori, Y.; Konishi, H.; Futamura, T.; Murata, A.; Koga, O.; Sakurai, H.; Oguma, K. *Electrochim. Acta* **2005**, *50*, 5354.
(20) Tang, W.; Peterson, A. A.; Varela, A. S.; Jovanov, Z. P.; Bech, L.; Durand, W. J.; Dahl, S.; Norskov, J. K.; Chorkendorff, I. *Phys. Chem. Chem. Phys.* **2012**, *14*, 76.
(21) Li, C. W.; Kanan, M. W. *J. Am. Chem. Soc.* **2012**, *134*, 7231.
(22) Christophe, J.; Doneux, T.; Buess-Herman, C. *Electrocatalysis* **2012**, *3*, 139.
(23) Durand, W. J.; Peterson, A. A.; Studt, F.; Abild-Pedersen, F.; Norskov, J. K. *Surf. Sci.* **2011**, *605*, 1354.
(24) Nie, X.; Esopi, M. R.; Janik, M. J.; Asthagiri, A. *Angew. Chem., Int. Ed.* **2013**, *52*, 2459.
(25) Strasser, P.; Koh, S.; Anniyev, T.; Greeley, J.; More, K.; Yu, C.; Liu, Z.; Kaya, S.; Nordlund, D.; Ogasawara, H.; Toney, M. F.; Nilsson, A. *Nat. Chem.* **2010**, *2*, 454.
(26) Eiswirth, M.; Bürger, J.; Strasser, P.; Ertl, G. *J. Phys. Chem.* **1996**, *100*, 19118.
(27) Rossmeisl, J.; Ferrin, P.; Tritsaris, G. A.; Nilekar, A. U.; Koh, S.; Bae, S. E.; Brankovic, S. R.; Strasser, P.; Mavrikakis, M. *Energy Environ. Sci.* **2012**, *5*, 8335.
(28) Abe, T.; Swain, G.; Sashikata, k.; Itaya, K. *J. Electroanal. Chem.* **1995**, *382*, 73.
(29) Aramata, A. Underpotential Deposition on Single-Crystal Metals. In *Modern Aspects of Electrochemistry*; Bockris, J. O. M., White, R. E., Conway, B. E., Eds.; Academic Press: New York, 1997; Vol. *31*; pp 181.
(30) Gasteiger, H. A.; Markovic, N. M.; Ross, P. N. *Abstr. Pap. Am. Chem. Soc.* **1995**, *210*, 296.
(31) Markovic, N.; Ross, P. N. *Langmuir* **1993**, *9*, 580.
(32) Shingaya, Y.; Matsumoto, H.; Ogasawara, H.; Ito, M. *Surf. Sci.* **1995**, *335*, 23.
(33) Bittner, A. M.; Wintterlin, J.; Ertl, G. *Surf. Sci.* **1997**, *376*, 267.
(34) Beitel, G.; Magnussen, O. M.; Behm, R. J. *Surf. Sci.* **1995**, *336*, 19.
(35) Xiao, X. Y.; Berenz, P.; Baltruschat, H.; Sun, S. *J. Electroanal. Chem.* **2001**, *500*, 446.
(36) Wonders, A. H.; Housmans, T. H. M.; Rosca, V.; Koper, M. T. M. *J. Appl. Electrochem.* **2006**, *36*, 1215.